Available online at www.sciencedirect.com
SCIENCE DIRECT
Polymer 47 (2006) 5080–5089
polymer
www.elsevier.com/locate/polymer

Diffusion of liquids in molten polymers: Mutual diffusion coefficient dependence on liquid miscibility and polymer molar mass

Redha Bella [a], Philippe Cassagnau [b], Françoise Fenouillot [a,*], Laurent Falk [c], Catherine Lacoste [d]

[a] *Laboratoire des Matériaux Macromoléculaires, Ingénierie des Matériaux Polymères IMP UMR-CNRS #5627, INSA of Lyon, 17 Avenue Jean Capelle, 69621 Villeurbanne Cedex, France*
[b] *Laboratoire des Matériaux Polymères et Biomatériaux, Ingénierie des Matériaux Polymères IMP UMR-CNRS #5627, Université Claude Bernard Lyon I, 15 Boulevard Latarjet, 69622 Villeurbanne Cedex, France*
[c] *Laboratoire des Sciences du Génie Chimique, ENSIC, 1 Rue Grandville BP 451 54001 Nancy, France*
[d] *Centre d'Etudes et de Recherche en Matériaux et Emballage, ESIEC, Esplanade Roland Garros, Technopôle Henri Farman BP 1029, 51686 Reims Cedex, France*

Received 9 January 2006; received in revised form 24 April 2006; accepted 11 May 2006
Available online 5 June 2006

Abstract

This paper addresses two important features of the diffusion of liquids into a molten polymer matrix: the dependence of the mutual diffusion coefficient on the liquid miscibility and molar mass of polymers. In addition, a rheological approach is chosen for its capacity to support modeling, and the mutual diffusion coefficient expressed with the free-volume theory, is estimated by an inverse method. For that purpose, the diffusion process of 2,3-epoxypropyl-phenylether (EPPE) and the *N*-ethylaniline (NEA) in three molten poly(ethylene-*co*-vinyle acetate) elastomers (EVA) having different molar masses is examined. The NEA is fully miscible with EVA and its diffusion process is not dependent on the molar mass of the polymer. On the other hand, the diffusion process of EPPE, that is partially miscible with EVA, is strongly influenced by the molar mass of the EVA. Furthermore, the evolution of the concentration gradient during the diffusion process of EPPE is driven by the necessity for the mixture to form a two-phase system with an EVA-rich phase and an EPPE-rich phase. In this case, the concentration gradient through the sample is not continuous at a macroscopic scale. Consequently, the calculation procedure is only applied during the early stages of the diffusion. For EPPE, the variation of the mutual diffusion coefficient with the molar mass of EVA is taken into account through the variation of the interaction parameter. Actually, despite the imperfections of the model, our experimental observations and rheological inverse calculation of the diffusion process are in agreement with the findings of the free volume theory of the diffusion.
© 2006 Elsevier Ltd. All rights reserved.

Keywords: Diffusion; Rheology; Modeling

1. Introduction

The diffusion of low molar mass organic molecules in molten polymers is involved in many operations such as mass polymerization processes, polymer modification, devolatilization, rubber formulation, plastification of thermoplastic polymers. More specifically in the field of reactive processing, the desired reaction is obtained provided that the reactants are able to diffuse at a molecular level to the reactive sites during the short period of time allowed for the process. Fortunately, the reactive processing equipments like twin-screw extruders are reactors that provide an intense mechanical mixing so that the distances of diffusion are considerably reduced by the mixing step. However, when large concentrations of a low viscosity liquid are mixed with high viscosity polymers, there may be some difficulties to achieve an efficient reduction of the characteristic size of the phases. In this particular case, it is essential to characterize diffusion rates to understand the overall reactive process. Self-diffusion coefficients can be determined by NMR such as the pulsed-gradient spin echo technique [1] but this technique requires nuclei solvents and it is not easy to determine diffusion coefficients in all samples at high temperatures characteristic of most polymer reactive processes. As experiments often have temperature and concentrations limitations, a solution is to calculate the mutual diffusion coefficient over a wide range of temperatures and concentrations from the free volume theory introduced first by Cohen and Turnbull [2]. In recent papers, several authors [3–5] have explained how to predict most of the parameters of the free volume theory so that it should be possible to calculate the

* Corresponding author. Tel.: +33 472438381; fax: +33 472438527.
E-mail address: francoise.fenouillot@insa-lyon.fr (F. Fenouillot).

0032-3861/$ - see front matter © 2006 Elsevier Ltd. All rights reserved.
doi:10.1016/j.polymer.2006.05.024

diffusion coefficient of small molecules in rubbery or glassy polymers. However, important assumptions must be made and consequently, the parameters are generally determined within one order of magnitude. We have demonstrated in a previous work that we were able to determine the mutual diffusion coefficient by comparing experimental rheological data collected during diffusion to values calculated from a model [6]. We have adjusted the values of three parameters of the free volume expression of the diffusion coefficient. Here, we wish to examine the influence of the miscibility of the species and of the molar mass of the polymer on the mutual diffusion coefficient. For that purpose, we have studied experimentally and modeled the diffusion behavior of 2,3-epoxypropylphenylether (EPPE) and of *N*-ethylaniline (NEA), two low molar mass molecules, in copolymers of ethylene and vinyl acetate (EVA) having different molar masses. The system EVA with EPPE and NEA is a model mixture that we have selected to analyze the relationships between mixing, diffusion and reaction in the context of reactive processing in polymer melts.

2. Diffusion process

The approaches to model the diffusion process are generally based on a dimensionless group called the relaxation diffusion Deborah number (θ_b), which is defined as the ratio of the characteristic time of the fluid, λ_m, to the characteristic time of the diffusion process, λ_D [7]:

$$\theta_b = \frac{\lambda_m}{\lambda_d} \tag{1}$$

The introduction of θ_b compares the rate of diffusion with the rate of conformational rearrangement of the macromolecules. If the Deborah number is large, the mass transport is called elastic diffusion. When the Deborah number approaches one, the molecular relaxation and mass transport processes occur in comparable time scales. The diffusion transport is then denoted as viscoelastic diffusion. In both cases, the diffusion does not follow a Fickian law. If the Deborah number is small, the polymer and solvent behave like purely viscous fluid. A solvent diffusing in a polymer at high temperature, above the glass transition temperature, or in a polymer containing a non-negligible fraction of solvent corresponds to that situation. In that case, mass transport can be described by the classical Fick's second law of diffusion:

$$\frac{\partial C}{\partial t} = \nabla D_{12} \nabla C \tag{2}$$

"C is the concentration of the diffusing molecule and is the del operator". D_{12} is the mutual diffusion coefficient that depends strongly on the concentration of the diffusing molecule.

3. Diffusion coefficient

A model that describes the diffusional transport of small molecules in macromolecules above their glass transition temperature (T_g) has been initiated by Cohen and Turnbull [1] and then extended by Vrentas and Duda [7–9]. The model establishes a relationship between the self-diffusion coefficient, D_1, of a molecule and the free-volume in a binary system. Recently, we have expressed D_1 in terms of specific volumes and flow activation energy derived from viscoelastic measurements [10,11]

$$D_1 = D_0 \exp\left(-\frac{E}{RT}\right) \exp\left[-\frac{\frac{\omega_1}{1+RT/E_1} V_1^T + \xi \frac{\omega_2}{1+RT/E_2} V_2^T}{\frac{\omega_1}{1+E_1/RT} V_1^T + \frac{\omega_2}{1+E_2/RT} V_2^T}\right] \tag{3}$$

D_0 is a constant, E is the critical energy necessary for a molecule to overcome attractive forces, V_i^T is the specific volume of specie i, at temperature T, ω_1 and ω_2 are the weight fractions of the solvent and the polymer, respectively, ξ is the molar volume ratio for the solvent and polymer jumping units. γ parameter is assumed to be 1 for the small molecule and for the polymer and therefore, does not appear in this equation.

The Flory–Huggins theory enables to derive the mutual binary diffusion coefficient, D_{12}, from the self-diffusion coefficient D_1. The expression of D_{12} is then

$$D_{12} = D_1 (1-\Phi_1)^2 (1-2\chi\Phi_1) \tag{4}$$

with Φ_1 the volume fraction of the solvent in the polymer and χ the Flory–Huggins interaction parameter.

The dependence of the diffusion coefficient on polymer molar mass, i.e. melt viscosity, is rarely studied experimentally at high temperature. Thus, it is important to point out that the free volume theory predicts that the self-diffusion coefficient is only dependent on the fractional free volume, i.e. on the temperature gap between the experimental temperature and T_g for a liquid/polymer system. Consequently, a molar mass dependence of the self-diffusion coefficient could be found only for non entangled polymer systems for which the T_g increases with increasing the molar mass. On the other hand, Eq. (4) shows that the mutual diffusion coefficient depends on the Flory–Huggins interaction parameter, which represents the interactions between the solvent and the polymer. Since, the solubility parameter is generally assumed to be independent on the molar mass for polymers, the mutual diffusion coefficient should be constant regarding the molar mass, i.e. the melt viscosity. However, Petri and Wolf [12] reported that the Flory–Huggins parameters depend on molecular weight even at high polymer concentrations, in contrast to the general belief according to which the individuality of macromolecules should already vanish in the region of moderate polymer concentrations.

4. Rheology and modelling scheme

4.1. Experimental setup for diffusion and rheology

The principle of the rheological experiment for diffusion was described in detail by Joubert [6] and its principle is presented in Fig. 1. A layer of liquid is placed on the top of a layer of molten polymer and the complex shear modulus ($G^*(\omega) = G'(\omega) + jG''(\omega)$) of the sample at a constant

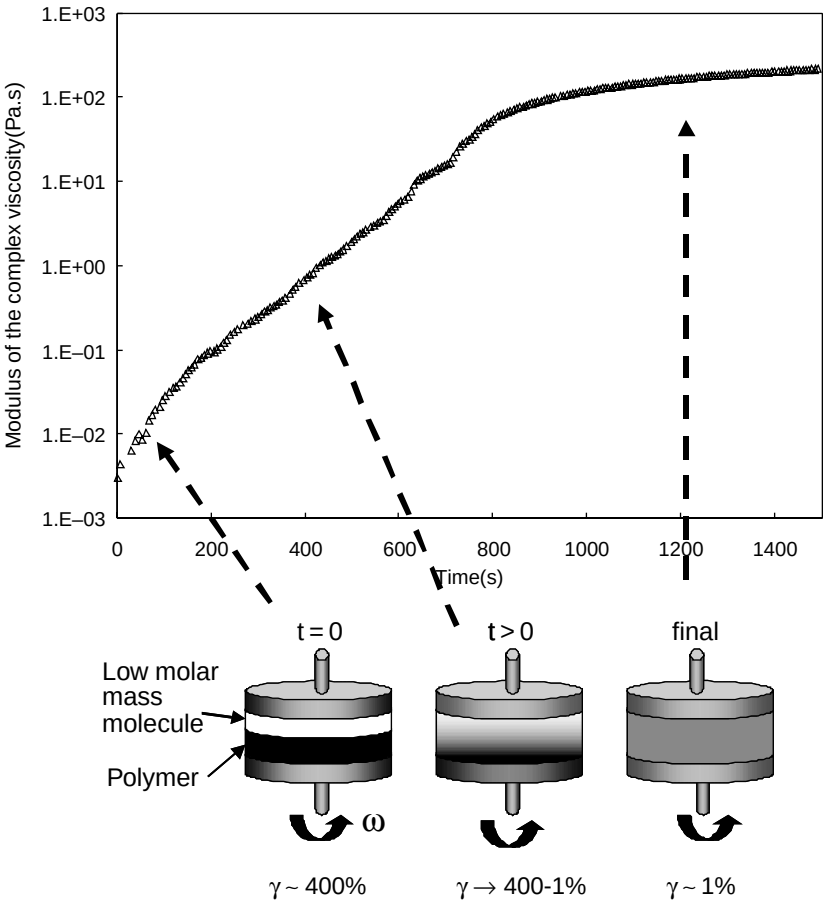

Fig. 1. Illustration of the evolution of the viscosity with the progress of the diffusion. The range of deformation used, γ, is indicated.

frequency ($\omega = 10$ rad s^{-1}) is measured as a function of time. In the present paper, we will consider the variation of the absolute complex viscosity, named for a convenient purpose viscosity.

$$|\eta * (\omega)| = \sqrt{\frac{G'^2}{\omega^2} + \frac{G''^2}{\omega^2}} \tag{5}$$

At the early stages of diffusion, the viscosity of the bi-layer is low since it is dominated the fluid of lower viscosity. In the intermediate stages, the diffusion of the low molar mass molecule across the polymer layer creates a gradient of concentration that induces viscosity variations. The global viscosity of the sample rises and finally, at the end of the diffusion process, the sample homogenizes and the viscosity reaches a stable value. The viscosity varies considerably from the viscosity of the liquid at the beginning of the diffusion process to the viscosity of the polymer–liquid homogeneous medium at the end of the diffusion process. Therefore, the evolution of the viscosity can be related to the transport behavior of the polymer–liquid system.

4.2. Diffusion process

The diffusion is supposed to occur in one direction perpendicular to the layer surface. The evolution of the concentration of the bi-layer specimen is calculated with Fick's law.

$$\frac{\partial C(t,x)}{\partial t} = \frac{\partial C}{\partial x}\left(D_{12}C(t,x)\frac{\partial C(t,x)}{\partial x}\right) \tag{6}$$

This requires to check that the process is Fickian by estimating the Deborah number, $\theta_b = \lambda_m/\lambda_D$. The relaxation time is equivalent to the reptation time of the EVA chains. Regarding the most unfavorable data for our calculation (longest relaxation time for the highest mass molar), for EVA 2803 at $T = 110$ °C, $\lambda_m \sim 10$ s. λ_m is expressed here as the longest average relaxation time of the distribution, $\lambda_m = \eta_0 J_e^0$. Note that the shortest time considered here according to data of Table 1 is $\lambda_m = \eta_0/G_N^0$ for EVA28800, so that $\lambda_m = 1.5 \times 10^{-4}$ s. η_0 is the zero shear viscosity, J_e^0 is the steady state compliance, G_N^0 is the rubbery modulus.

Table 1
Characteristics of penetrant liquids

Penetrant liquids	Molar mass (g mol^{-1})	η_0[a] (Pa s)	E_1[b] (kJ mol^{-1})
2,3-Epoxypropyl-phenylether (EPPE)	150	1.5×10^{-3}	30
N-Ethylaniline (NEA)	121	7×10^{-4}	30

[a] $T = 110$ °C.
[b] Calculated from EVA/amine blend according to Ref. [10].

The characteristic time of the diffusion, λ_D, is more difficult to estimate, Peppas et al. [13] proposed the following expression

$$\lambda_D \sim L^2/D_{12} \tag{7}$$

where L is the thickness of the polymer layer. According to our experimental conditions, $L \sim 10^{-3}$ m and according to our next calculation $D_{12} \sim 10^{-8}$ m^2 s^{-1} for a polymer volume fraction of 0.1, we find $\lambda_D \sim 10^2$ s. The Deborah number is therefore: $\theta_b \sim 10^{-1}$, which indicates that the process is fickian even for the most unfavorable case of calculation.

Those estimates show that the molecular relaxation is faster than the diffusive transport so that changes in the polymer conformations are not limiting the process and we have a viscous or liquid–liquid diffusion.

4.3. Inverse calculation

The difficulty for calculating the self-diffusion and mutual diffusion coefficients is that the expressions in Eqs. (3) and (4) require the determination of a number of parameters. Some of them are directly accessible: ω_1 and ω_2 are the weight fractions of the small molecules and the EVA, respectively. The specific volumes V_1^T and V_2^T at the temperature T were calculated from the experimental determination of the volume of the NEA and of the EPPE at 90, 110, 130 and 150 °C. The following relations were established:

$$V_1^T = 0.93104 \exp(2.203 \times 10^{-5}\, T^{3/2})\ \text{cm}^3\ \text{g}^{-1} \text{ for the NEA} \tag{8}$$

$$V_1^T = 0.80344 \exp(2.218 \times 10^{-5}\, T^{3/2})\ \text{cm}^3\ \text{g}^{-1} \text{ for the EPPE} \tag{9}$$

The specific volume of the EVA28 was measured by Rodgers [14], it is equal to:

$$V_2^T = 1.00832 \exp(2.241 \times 10^{-5}\, T^{3/2})\ \text{cm}^3\ \text{g}^{-1} \tag{10}$$

E is generally considered to be zero. E_1 and E_2 are the flow activation energies of the low molar mass molecule and the EVA, respectively, their determination is based [10] on the measurement of the viscoelastic properties of the EVA alone and of the binary mixtures of EVA with NEA and with EPPE (Tables 1 and 2). In first approximation, the Flory–Huggins parameter, χ, can be estimated according to the following equation

$$\chi = 0.34 + \frac{V}{RT}(\delta_1 - \delta_2)^2 \tag{11}$$

where V is the molar volume of the penetrant liquid, δ_1 and δ_2 are the solubility parameters of the liquid and the polymer, respectively. According to the Van Krevelen method [15] we find $\chi \approx 0.40$ for the EVA/NEA and $\chi \approx 0.50$ for EVA/EPPE systems. It must be pointed out that higher values of χ are obtained from Hoy method [15]. In the present work, we use Van Krevelen reference ($\chi_{NEA/EVA} \approx 0.40$). Regarding EPPE/EVA system, the value of the Flory–Huggins parameter will be discussed later from the procedure modeling point of view.

Table 2
Viscoelastic parameters of EVA samples determined from the master curve (time–temperature superposition) of the complex shear modulus at the reference temperature $T_0 = 110$ °C

Polymer	Melt flow index	M_w (g mol^{-1})	J_e^0 (Pa^{-1})	η_0 (Pa s)	E_2 (kJ mol^{-1})
EVA 2803	3	53,500[a]	2.0×10^{-4}	5.0×10^{4}	44.5
EVA 2840	40	27,500[b]	0.9×10^{-4}	5.2×10^{3}	45.8
EVA 28800	800	7900[b]	1.1×10^{-4}	75	38.0

The plateau modulus G_N^0 was taken equal to 5×10^5 Pa according to Ref. [23].
[a] From Ref. [23].
[b] From rheological calculation assuming $M_w \propto \eta_0^{1/3.4}$ for entangled polymers.

Eventually, only D_0 and ξ, need to be fitted with the help of the diffusion and rheological model to express the mutual coefficient of diffusion. At the beginning of the calculation, we assume values for the parameters D_0 and ξ of the diffusion model in order to calculate D_{12}. D_{12} is needed to calculate the evolution of the concentration through the sample. The knowledge of the concentration allows to deduce the viscosity profile and to derive the viscosity of the overall sample at each time, referring to a theoretical framework of the dilution effect [10,16]. The next step is to compare the calculated viscosity evolution to the experimental one and subsequently modify D_0 and ξ to obtain the best adjustment of the variation of the viscosity. The method can be assimilated to a rheological inverse calculation method since the parameters of the free volume expression of the diffusion coefficient are calculated by comparing the experimental viscosity versus time curve to the values calculated from the rheological model. This method was described in details by Joubert et al. [6] and we use the software developed by these authors. However, the numerical method is based on a fundamental assumption of liquid–polymer diffusion in the gap of the rheometer plates. This assumption must be actually checked in the present work. As shown in Fig. 2, the thickness of the solid is initially divided into $(n-1)$ equal slices and the liquid fills the last nth slice

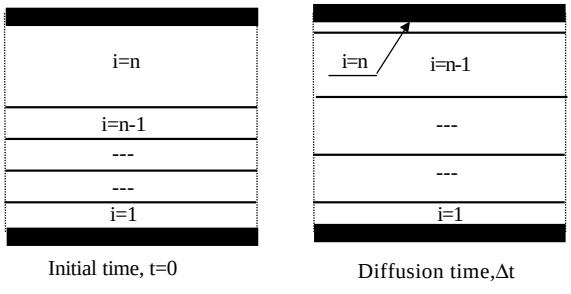

Fig. 2. Schematic description of the diffusion process for numerical purpose. The upper layer ($i=n$) is considered to be composed of pure liquid until it is reduced to 0.01% of the gap, it is then suppressed.

completely. According to the additivity of the volumes of the solid and of the liquid, the polymer swells as the liquid gets into a slice. Thus, the thickness of each 'solid' slice increases over diffusion time whereas the liquid one decreases. The assumption considered that, when the abscissa of the last slide (upper slide $i=n-1$) of the 'solid' reaches 99.99% of the gap, the swelled polymer occupies the overall gap and there is no more free liquid above it. In computation, the last slice corresponding to liquid $i=n$ is then suppressed and the diffusion of liquid continues inside the polymer until the equilibrium is achieved.

Actually, this assumption means that the penetrant liquid diffuses in the polymer, which swells and the polymer chains does not diffuse in the pure liquid slice. In other words, there is no dissolution effect of polymer in the upper nth slice. This assumption can be discussed from the comparison between the diffusion coefficient of the liquid D_{12} and the diffusion coefficient of the polymer D_p. We can then define a diffusion Deborah number as:

$$\mathcal{D}_b = D_p/D_{12} \tag{12}$$

If $\mathcal{D}_b$ is lower than 1, the solvent penetration rate is faster than the polymer dissolution rate. D_{12} is calculated a posteriori in the present work. According to the reptation theory D_p can be expressed for bulk conditions as following

$$D_p = \frac{\langle R^2\rangle_0}{\pi^2 T_d} \tag{13}$$

where $\langle R^2\rangle_0$ is the unperturbed mean-square end-to-end distance of the polymer chain. T_d is the reptation time and can be assimilated to λ_m. For semi-diluted and concentrated solutions T_d is expressed as

$$T_d(\Phi_2) = a_\Phi \Phi_2^{1.75} T_{d\ bulk} \tag{14}$$

Where Φ_2 is the volume concentration of polymer in the penetrant liquid, a_Φ is the free volume correction that takes into account the change of the glass temperature with dilution Φ_2, T_{dbulk} is the reptation time of the bulk polymer at the temperature considered.

$\langle R^2\rangle_0$ was calculated according to Fetters et al. [17] who proposed a direct and simple relation between the various viscoelastic parameters and chain packing length. We used data on polyethylene so that $\langle R^2\rangle_0/M=1.25$ ($\text{Å}^2\,\text{mol}\,\text{g}^{-1}$). Using the most unfavorable conditions (EVA28800) in concentrated conditions at $T=110$ °C ($\Phi_2\to1$, $a_\Phi\approx1$, $T_d=1.5\times10^{-4}$ s) we find $D_p\approx7\times10^{-14}\,\text{m}^2\,\text{s}^{-1}$ and $D_{12}\approx7\times10^{-14}\,\text{m}^2\,\text{s}^{-1}$ (Fig. 9, $\omega_1\to0$) so that $\mathcal{D}_b\approx1$. Actually the most unfavorable condition for polymer diffusion at $T=110$ °C should be at $\Phi_2=0.5$ (EVA28800, $T_d(\Phi_2=0.5)\approx1\times10^{-5}$ s according to Eq. (14) with $a_\Phi=0.25$), consequently $D_p\approx5\times10^{-13}\,\text{m}^2\,\text{s}^{-1}$. However, $D_{12}\approx10^{-9}\,\text{m}^2\,\text{s}^{-1}$ (Fig. 9) so that $\mathcal{D}_b\approx5\times10^{-4}$. Therefore, due to the fact that D_{12} is more sensitive to the variation of polymer concentration than D_p, the most unfavorable case is obtained with $\Phi_2\to1$. The most favorable conditions (EVA2803, $T_d=1\times10^{-1}$ s) with $D_p\approx7\times10^{-16}\,\text{m}^2\,\text{s}^{-1}$ and $D_{12}\approx7\times10^{-14}\,\text{m}^2\,\text{s}^{-1}$ leads to $\mathcal{D}_b\approx10^{-2}$. This simple calculation shows that $10^{-2}<\mathcal{D}_b<10^{0}$ for EVA samples investigated in the present work so that the dilution effect of the polymer can be neglected. Indeed, the diffusion Deborah number shows that the solvent penetration rate is much higher than the dissolution rate. According to this result, the hypothesis of the upper n slice containing pure liquid and decreasing with diffusion time is correct.

5. Experimental

5.1. Materials and samples

The polymers used are three poly(ethylene-*co*-vinyle acetate) (EVA) with different molar masses, i.e. melt viscosity (Table 1). The samples were kindly supplied by Arkema. The amount of acetate groups contained in these copolymers is 28 wt%. The organic molecules are the 2,3-epoxypropyl-phenylether (EPPE) and the *N*-ethylaniline (NEA) purchased from Aldrich and used without further purification.

5.2. Viscoelastic measurements

The zero shear viscosities of the liquids, NEA and EPPE, have been measured on a stress rheometer from TA Instruments (AR 1000) on shear steady regime at 90, 110, 130 and 150 °C.

For the viscoelastic characterization of the pure polymers, frequency sweep test were run from 10^{-1} to $10^{2}\,\text{rad}\,\text{s}^{-1}$ at different temperatures, 90, 110, 130, 150, 170 at 190 °C on a Rheometrics Mechanical Spectrometer (RMS800). The terminal viscoelastic parameters (Table 2) of the three EVA grades were deduced from the time–temperature superposition of the viscosity curves at the reference temperature of 110 °C.

For the diffusion experiments, parallel plate geometry with a diameter of 50 mm was mounted on the RMS800. The tests were run in dynamic conditions at $10\,\text{rad}\,\text{s}^{-1}$, and four temperatures were experimented: 90, 110, 130 and 150 °C. A disc of EVA was prepared by compression molding and its thickness was precisely measured. It was brought into contact with the lower plate heated at 110 °C. The liquid additive was deposited over the polymer layer. The upper plate was then lowered in order to respect a gap of 2 mm between the plates. The thickness of the EVA was equal to 0.9 mm and the thickness of the liquid was equal to 1.1 mm. The strain amplitude was manually adjusted from 400% at the beginning of the test to 1% at the end of the experiment to obtain a measurable torque and to remain within the domain of linear viscoelasticity.

5.3. Size exclusion chromatography (SEC)

The composition of EVA/EPPE mixture phases was determined by size exclusion chromatography (SEC) after reaching the thermodynamic equilibrium of the mixture placed in a glass tube at controlled temperature. A sample of the two distinct phases was taken from the upper and lower sections of the tube and analyzed. The apparatus was a Viscotek

chromatograph for low molecular weight polymers with two ViscoGEL® HR High Resolution Columns (pores diameter ~100–500 nm). The elution solvent was tetrahydrofurane (THF). The refractive index peaks, measured using a Viscotek VE 3580 RI detector, were integrated and the EPPE concentration deduced thanks to a calibration curve prepared with EPPE/THF solutions of known concentration. The calibration of the apparatus was made with polystyrene standards.

6. Results and discussion

Prior to the results, it is interesting to examine the sensitivity of the model to variations of its parameters, D_0, ξ, and χ. The viscosity evolutions for different sets of parameters varying independently one from each other have been calculated for NEA and EPPE diffusing in EVA at 110, 130 and 150 °C. In Figs. 3 and 4, we have selected several representative examples of the variations of the model calculations. In all cases, the viscosity evolution of the EPPE/EVA systems was more sensitive to variations of the parameters than that of NEA/EVA.

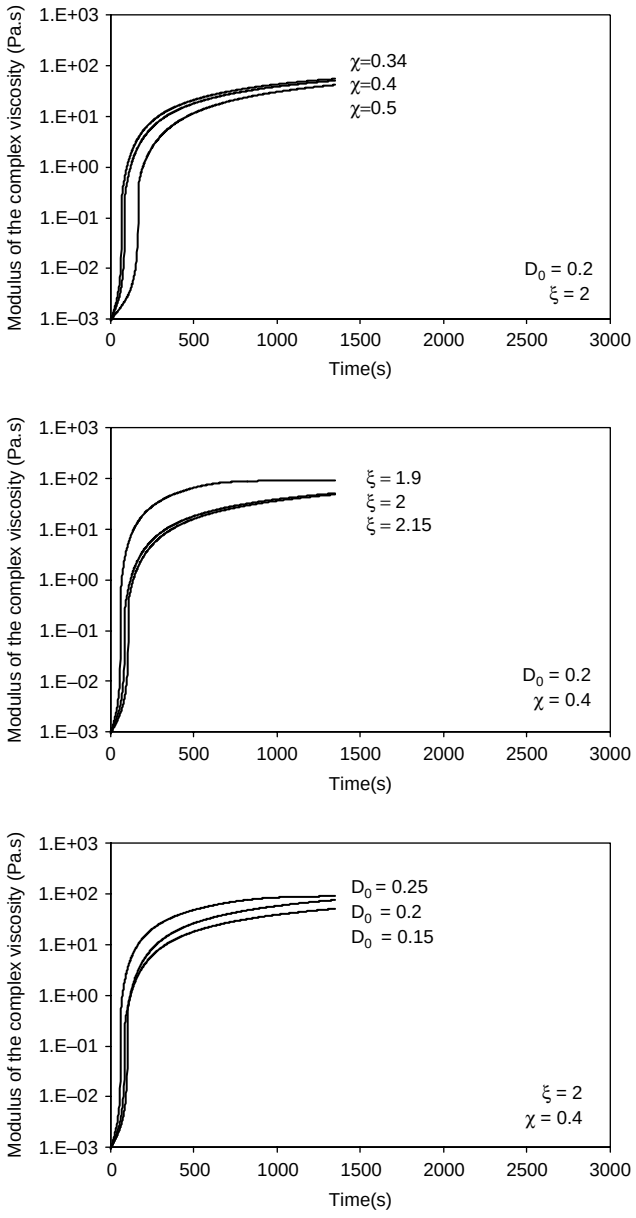

Fig. 3. Sensitivity of the calculated viscosity to the variations of the D_0, ξ and χ parameters for NEA/EVA2840 bi-layer at 130 °C.

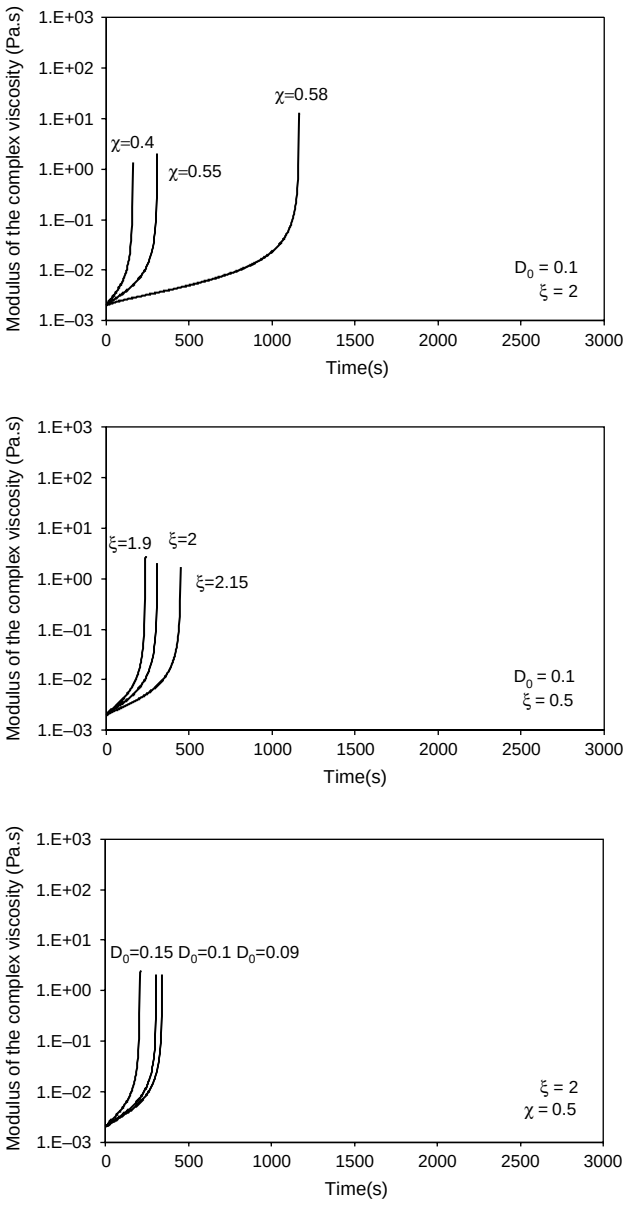

Fig. 4. Sensitivity of the calculated viscosity to the variations of the D_0, ξ and χ parameters for EPPE/EVA2840 bi-layer at 130 °C.

6.1. Diffusion of NEA in EVA samples

It must be pointed out that the NEA was found to be miscible in all proportions with the different grades of EVA at 110 °C. The evolution of the viscosity at different temperatures of the NEA/EVA2840 bi-layer is shown in Fig. 5. The absolute viscosity varies considerably from absolute viscosity of NEA liquid at the beginning of the diffusion process compared to the

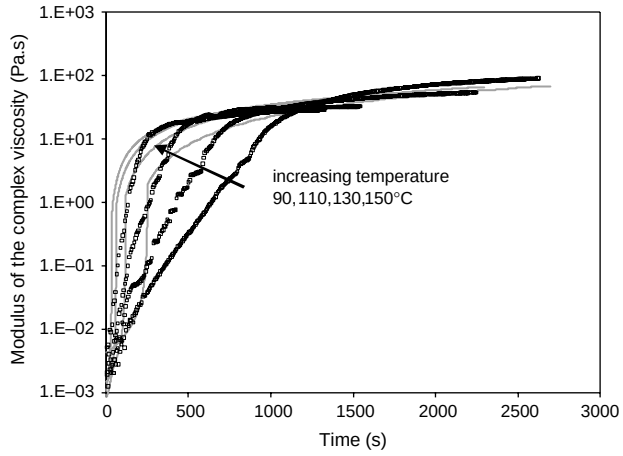

Fig. 5. Evolution of the viscosity of the NEA/EVA2840 bi-layer at different temperatures, $T=90$, 110, 130 and 150 °C. Symbols: experimental data, continuous line: prediction of the diffusion model. D_0, and ξ have been optimized by inverse calculation with the experimental data at 110 °C for EVA2840 only. Then their values ($D_0=0.2$ m^2/s and $\xi=2$) were integrated in the model to simulate all the other experiments with variable temperature and variable molar mass of the EVA (Fig. 6).

absolute viscosity of EVA2840-NEA homogeneous medium at the end of the diffusion process. Furthermore, the rate of diffusion is obviously activated by an increase of temperature. The diffusion process of the amine is completed after 2500 s at 90 °C whereas it is finished after 100 s at 150 °C. Actually, the influence of temperature is clearly illustrated on the initial slope of the viscosity plot. The diffusion rate is enhanced by increasing temperature as predicted by Eq. (3). On the other hand, Fig. 6 shows the evolution of the absolute viscosity for EVA samples having different mass molar at $T=110$ °C. Interestingly, the evolution of the viscosity before reaching the final plateau is similar for all samples. In other words, the slopes of the viscosity versus time curves are the same regardless of the molar mass of the EVA. This feature indicates that the kinetics of NEA diffusion does not depend on EVA molar mass. Moreover, the time necessary to attain a stabilized

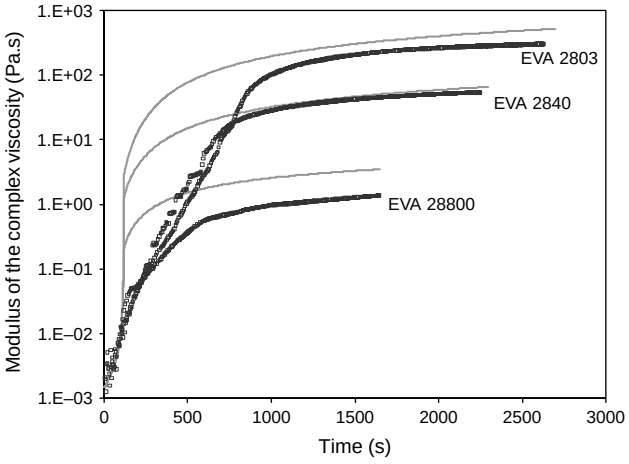

Fig. 6. Evolution of the viscosity of the NEA/EVA bi-layer at 110 °C for different molar masses of the EVA. Symbols: experimental data, continuous line: prediction of the diffusion model. See comments in legend of Fig. 5.

value of the viscosity is equivalent for the three samples. Only the value of the final viscosity varies, as a consequence of the difference in molar masses.

We have applied the model in order to determine the parameters of the diffusion coefficient expression. The parameters D_0, and ξ have been optimized with the experimental data collected at 110 °C only. Their values ($D_0=0.2$ m^2/s and $\xi=2$) were integrated in the model to simulate all the other experiments with variable temperature and variable molar mass of the EVA. Examples of calculated viscosities are shown in Figs. 5 and 6. It can be seen that the model mainly captures the initial and final features of the experimental plots, whereas the actual global kinetics of diffusion is slower than modeled. Some assumptions can be revisited for this. First some limits of the free volume diffusion models can be put forward, as it was done recently [3,5]. For example, the critical energy E is presently set equal to zero, whereas the model was shown to be very sensitive to its value [5]. The experimental and computed plots are in better agreement at 150 °C than 90 °C (Fig. 5). This is consistent with the fact that energy effects are all the more dominant over free volume effects as temperature increases [3]. On the other hand, the original framework of the free volume theory assumes the additivity of free volumes; this hypothesis is generally a rough approximation although it is always assumed in all literature devoted to the free volume theory for diffusion [18]. The poor agreement between the calculated and experimental viscosities at the intermediate stage of diffusion might be due to the amine dissolving the EVA so that the model of an upper layer being pure liquid is not representing adequately the actual process. This possible aspect was discussed in term of the diffusion Deborah number (Eq. (12)). Our previous discussion showed that the polymer disentanglement from bulk phase to the liquid upper layer is not the dominant mode. Indeed, our experimental results (Fig. 6) confirm our hypothesis since the viscosity variation at the earlier stage of diffusion is not molar mass dependent. Assuming a disentanglement process would lead to a molar mass dependence of the viscosity due to the fact that a short chain disentangles faster than a longer.

In spite of these reservations, the physical significance of the calculated D_0 and ξ is demonstrated here by the fact that equally satisfactory, or even better prediction can be achieved (Eq. (3)) at different temperatures while keeping the values of these parameters constant, as expected.

The parameters of Eqs. (3) and (4) being known, it is finally possible to calculate in one hand the self-diffusion coefficient D_1 (Eq. (4)) and on the other hand the mutual diffusion coefficient D_{12} (Eq. (4)) versus the volume fraction of the polymer at any temperature (Fig. 7).

6.2. Diffusion of EPPE in EVA samples

The evolution of the viscosity at different temperatures of the EPPE/EVA2840 bi-layer is shown in Fig. 8. As previously reported, the absolute viscosity varies considerably from absolute viscosity of the EPPE liquid at the beginning of the diffusion process to the absolute viscosity of EPPE/EVA2840

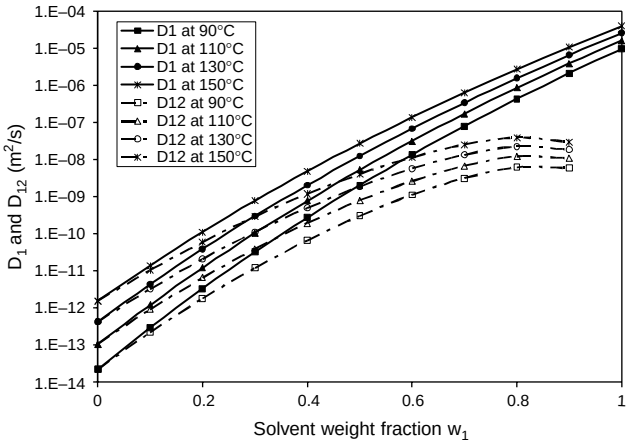

Fig. 7. Calculated variation of the self-diffusion coefficient D_1 and mutual coefficient D_{12} versus solvent weight fraction at different temperatures for NEA/EVA2840 system.

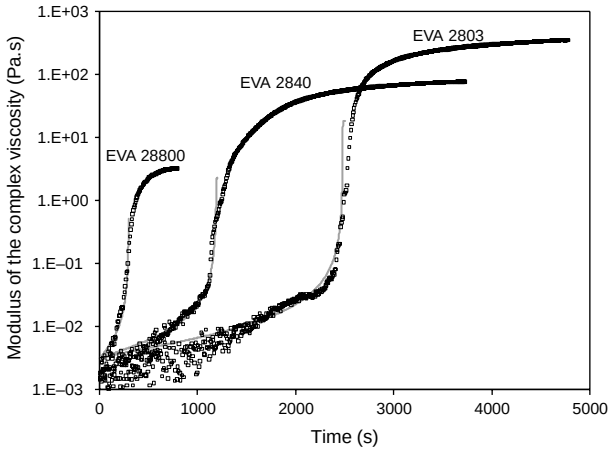

Fig. 9. Evolution of the viscosity of the EPPE/EVA bi-layer for different molar masses of the EVA. Symbols: experimental data, continuous lines: prediction of the diffusion model. Prediction of the diffusion model for EPPE/EVA system. χ, D_0, and ξ have been optimized by inverse calculation with the experimental data at 110 °C for EVA2840. Then the values $D_0=0.1$ m^2/s and $\xi=2$ were kept constant and integrated in the model to simulate all the other experiments by fitting χ (see Table 3).

equilibrium medium at the end of the diffusion process. Qualitatively, the apparent rate of diffusion of EPPE in EVA is two to five times slower than that of the NEA in EVA. Nevertheless, the trend of the diffusion curve is quite different compared with NEA/EVA system and especially at low temperature ($T=90$ °C). The diffusion curve is separated in two distinct behaviors. The first part of the curve shows a slow variation of the viscosity with diffusion time whereas the second part of the curve shows a strong increase of the viscosity towards the final equilibrium plateau. Also, the apparent rate of diffusion is more strongly activated by the temperature compared with NEA/EVA system. Moreover, Fig. 9 shows by contrast with Fig. 6 that the diffusion rate of the EPPE depends strongly on the molar mass of the polymer. The explanation for such different behaviors is linked to differences in the solubility of the two small molecules in EVA. Actually, EPPE is only partially miscible with the EVAs, with an Upper

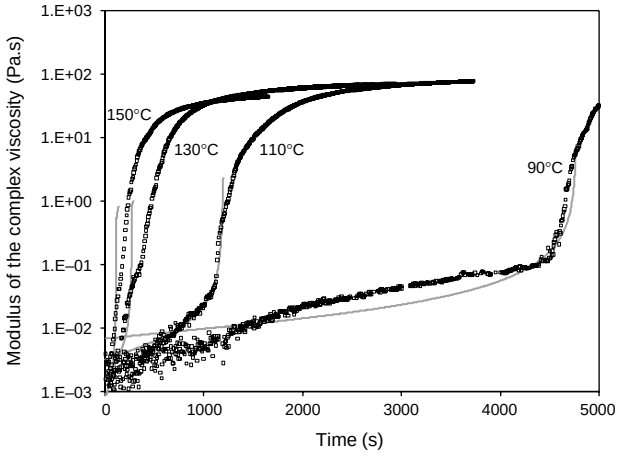

Fig. 8. Evolution of the viscosity of the EPPE/EVA2840 bi-layer at different temperatures, $T=90$, 110, 130 and 150 °C. Symbols: experimental data, continuous line: prediction of the diffusion model. Prediction of the diffusion model for EPPE/EVA system. χ, D_0, and ξ have been optimized by inverse calculation with the experimental data at 110 °C for EVA2840. Then the values $D_0=0.1$ m^2/s and $\xi=2$ were kept constant and integrated in the model to simulate all the other experiments by fitting χ (see Table 3).

Critical Solution Temperature (UCST). At 110 °C, a mixture of EVA with EPPE forms a two phase system with one phase rich in EVA and the other rich in EPPE. The equilibrium compositions at 110° (with EVA 28800) of the EPPE-rich phase and of the EVA-rich phase are, respectively, 66 and 26 wt% of EPPE as determined by SEC.

The interdiffusion at the interface between partially miscible binary liquid–liquid systems has been studied for a long time in the case of low molar mass species [19,20]. In the case of polymers, the behavior of interfaces in non-equilibrium conditions, that is when a macroscopic mass transfer exists at long distance, is not perfectly understood. When two fluid layers are put into contact and heated at a temperature below their critical temperature, the initially sharp interface broadens in the early stage of the interdiffusion. For polymer/polymer systems, the thickness of the interface, w, stabilizes around 100 nm [21,22], a value that is probably higher for a polymer/solvent system. Then, the interface is being crossed by a macroscopic mass flow until the equilibrium concentrations, C_{1eq} and C_{2eq}, are attained in the phases (Fig. 10). The concentration of the phases has to reach its equilibrium value by means of a diffusion process. In other words, compared to a fully miscible system, the molecular transport is not only driven by the necessity to homogenize the mixture, but also by the necessity to create two distinct phases. The sample may be viewed as two macroscopic layers where a classical Fickian transport occurs, separated by a thin interface where the concentration profile is very sharp. Note also that when one of the species diffuses faster than the other, or if the global concentration of the species is different from the critical composition, the interface shifts toward the side of the faster diffusion component or toward the minor component. To summarize, for our particular system, the partial immiscibility of EPPE in EVA influences deeply the profile of concentration

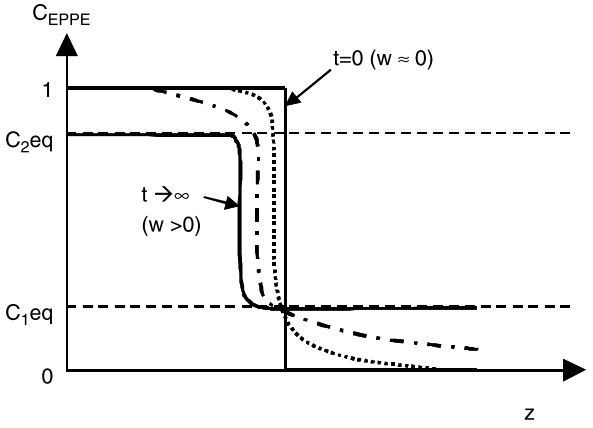

Fig. 10. Schematic description of the concentration profiles of the partially miscible system. The coordinate z is the axis perpendicular to the bi-layer specimen. The initial condition consists of pure liquid upper layer separated from the pure polymer layer by a sharp interface ($t=0$, $w=0$). For late times ($t\rightarrow\infty$) the equilibrium concentration profile is established with a liquid-rich layer of concentration C_{2eq} and a polymer-rich layer of concentration C_{1eq}. The thickness of the interface, w, has increased ($w>0$). The non-equilibrium profiles are represented at two intermediate stages (dashed curves). Since, the liquid diffuses much faster than the polymer chains, the concentration gradient in the polymer establishes faster than in the liquid layer.

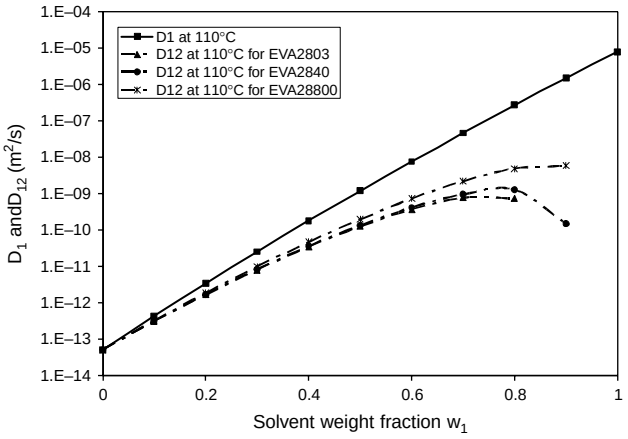

Fig. 11. Calculated variation of the self-diffusion D_1 and mutual D_{12} coefficients versus solvent weight fraction at $T=110\,^{\circ}C$ for EPPE/EVA systems with EVAs of different molar masses (EVA2803, EVA2840 and EVA28800).

produced. We can no longer consider a continuous variation of concentration.

Although the mass transfer on both sides of the interface region is classical, it is difficult to say whether the existence of this interface between the phases, has an impact on the global rate of the diffusion process, and the literature does not indicate whether the molecular flow having to cross the interface is slowed down. In our case this is of importance since the diffusion process takes longer time for the EPPE than for the NEA. But this feature might be linked to other parameters like the hydrodynamic volume of the molecules and their interactions with EVA as it will be discussed further.

Despite the partial miscibility of EPPE, the evolution of the viscosity of the bi-layer is able to represent the rate of the diffusion process. The reason is that the liquid EPPE layer thickness is decreasing consequently to the mass transfer and this decrease dominates the measured viscosity as explained in the section presenting the inverse calculation method. Therefore, the rheological model that decomposes the sample disk in layers with the upper layer being pure liquid is valid as long as the interface between the EPPE-rich phase and the EPPE does not reach the upper boundary of the specimen, which is the upper plate. Therefore, the model was applied to EPPE/EVA systems and the evolution of the experimental and calculated viscosities is depicted in Figs. 8 and 9, with different operating temperatures, and different molar masses of the EVA, respectively. It is interesting to note that a correct agreement of the calculated viscosity with the experiment was obtained only if the interaction parameter, χ, depended on the molar mass of the polymer (Table 3). Actually, the variations of χ reflects well the behavior of EPPE/EVA binary mixtures, that have an upper critical solution temperature and which miscibility window is enlarged for a lower molar mass of the polymer. The other parameters of the model were found to be: $D_0=0.1\ m^2\ s^{-1}$ and $\xi=2$. The variations of D_1 and D_{12} at $T=110\,^{\circ}C$ are plotted in Fig. 11.

Table 3
Parameters of the diffusion model

NEA/EVA system		
Parameters for all temperatures and EVAs		
$D_0=0.2\ m^2\ s^{-1}$, $\xi=2$, $\chi=0.4$		
EPPE/EVA system		
Parameters for all temperatures and EVAs		
$D_0=0.1\ m^2\ s^{-1}$, $\xi=2$		
Parameters depending on the molar mass		
EVA 28800	EVA 2840	EVA 2803
$T=110\,^{\circ}C$, $\chi=0.34$	$T=90\,^{\circ}C$, $\chi=0.58$	$T=110\,^{\circ}C$, $\chi=0.58$
	$T=110\,^{\circ}C$, $\chi=0.55$	
	$T=130^{\circ}C$, $\chi=0.5$	
	$T=150\,^{\circ}C$, $\chi=0.46$	

7. Conclusion

In this paper, we investigated the diffusion of organic molecules in molten EVAs of different molar masses, from original rheological experiments. Two different organic molecules were chosen to study the dependence of the mutual diffusion coefficient on the Flory–Huggins interaction parameter. The diffusion process of the amine (*N*-ethylaniline, NEA), that is miscible with the polymer, was not dependent on the molar mass of the EVA. By contrast with the amine, the diffusion process of the epoxy (2,3-epoxypropyl-phenylether, EPPE), partially miscible with the EVA, depended strongly on the molar mass of the EVA. It is to be noticed that the diffusion process for this latter molecule is complex. The epoxy/EVA sample formed a two-phase system with a concentration profile that was not continuous at a macroscopic level. However, the hypothesis of the late persistence of a layer of pure epoxy in contact

with the upper plate allowed to simulate the viscosity evolution until the EVA diffusion front reaches the boundary of the sample.

Rheology proved to be a very sensitive tool to follow experimentally diffusion, however, the calculation developed from a rheological inversion method relies on several assumptions and consequently, the representation of the experimental data was imperfect. As a consequence, fitting a model of Fickian diffusion to our rheological measurements enables to obtain only estimations of the mutual diffusion coefficient of the polymer/liquid system. Despite that point, the trends of our experimental observations and rheological inverse calculation of the diffusion process are in agreement with the general finding of the free volume theory of diffusion. Indeed, the mutual diffusion coefficient of the amine in EVA was found to be constant regardless EVA molar mass. This leads to the conclusion that the Flory–Huggins parameter does not depend neither on EVA mass molar and neither on temperature for the amine/EVA system. For EPPE, the self-diffusion coefficient, D_1, was found to depend on the liquid volume fraction and on temperature. Actually, only the mutual coefficient diffusion, D_{12}, depends on the molar mass of EVA through the dependence of the Flory–Huggins interaction parameter.

It is the first time that such experimental investigations on molten polymer aimed to verify the free volume theory of diffusion of liquid in molten polymers. This is a key issue in further prospects of predicting the balance between reaction and diffusion in reactive systems involving molten polymers since our study shows that the mutual coefficient diffusion depends strongly on the volume fraction of diffusing molecules.

Acknowledgements

Dr D. Sage is gratefully acknowledged for his help in calculating the solubility parameters of the components of our systems.

References

[1] Pickup S, Blum F. Macromolecules 1989;22:3961–8.
[2] Cohen MH, Turnbull D. J Chem Phys 1959;31:1164.
[3] Zielinski JM, Duda JL. AIChE J 1992;38:405–15.
[4] Vrentas JS, Vrentas CM. Eur Polym J 1998;34(5/6):797–803.
[5] Tonge MP, Gilbert RG. Polymer 2001;42:1393–405.
[6] Joubert C, Cassagnau P, Michel A, Choplin L. J Rheol 2002;46(3): 629–50.
[7] Vrentas JS, Duda JL. J Polym Sci, Part B: Polym Phys 1977;15:403–16.
[8] Vrentas JS, Duda JL. J Polym Sci, Part B: Polym Phys 1977;15:417–39.
[9] Vrentas JS, Duda JL. J Polym Sci, Part B: Polym Phys 1977;15:440–53.
[10] Gimenez J, Michel A, Cassagnau P. J Rheol 2000;44:527–47.
[11] Ponsard-Fillette M, Barrès C, Cassagnau P. Polymer 2005;46:10256–68.
[12] Petri HM, Wolf BA. Macromol Phys 1995;196:2321–33.
[13] Peppas NA, Wu JC, Von Meerwall ED. Macromolecules 1994;27(20): 5626–38.
[14] Rodgers PA. J Appl Polym Sci 1993;48:1061–80.
[15] Barton Allan FM. Handbook of solubility parameters and other cohesion parameters. 2nd ed. Boca Raton: CRC Press Inc.; 1991.
[16] Marin G, Menezes E, Raju VR, Graessley WW. Rheol Acta 1980;19:462.
[17] Fetters LJ, Lohse DJ, Richter D, Witten TA, Zirkel A. Macromolecules 1994;27(17):4639–47.
[18] Ferry JD. Viscoelastic properties of polymers. New York: Wiley; 1980 p. 280.
[19] Perez de Ortiz ES, Sawistowski H. Chem Eng Sci 1973;28:2063–9.
[20] Aguirre FJ, Klinzing GE, Chiang SH, Leaf GK, Minkoff M. Chem Eng Sci 1985;40(8):1449–56.
[21] Bruder F, Brenn R, Stühn B, Strobl GR. Macromolecules 1989;22: 4434–7.
[22] Puri S, Binder K. Phys Rev B: Rapid Commun 1991;44(17):9735–8.
[23] Cassagnau P, Bert M, Verney V, Michel A. Polymer 1993;34:123–32.